



Published in final edited form as:

Circulation. 2005 August 9; 112(6): 885–892. doi:10.1161/CIRCULATIONAHA.104.520098.

Characterization of Atherosclerotic Plaques by Laser Speckle Imaging

Seemantini K. Nadkarni, PhD, Brett E. Bouma, PhD, Tina Helg, PhD, Raymond Chan, PhD, Elkan Halpern, PhD, Alexandra Chau, SB, Milan Singh Minsky, PhD, Jason T. Motz, PhD, Stuart L. Houser, MD, and Guillermo J. Tearney, MD, PhD

Department of Dermatology (S.K.N., B.E.B.), Department of Pathology (S.L.H., G.J.T.), and Department of Radiology (R.C., E.H.), Harvard Medical School, and Wellman Center for Photomedicine (S.K.N., B.E.B., T.H., R.C., A.C., M.S.M., J.T.M., G.J.T.), Massachusetts General Hospital, Boston, and Departments of Health Sciences and Technology (B.E.B.) and Mechanical Engineering (A.C.), Massachusetts Institute of Technology, Cambridge

Abstract

Background—A method capable of determining atherosclerotic plaque composition and measuring plaque viscoelasticity can provide valuable insight into intrinsic features associated with plaque rupture and can enable the identification of high-risk lesions. In this article, we describe a new optical technique, laser speckle imaging (LSI), that measures an index of plaque viscoelasticity. We evaluate the potential of LSI for characterizing atherosclerotic plaque.

Methods and Results—Time-varying helium-neon laser speckle images were acquired from 118 aortic plaque specimens from 14 human cadavers under static and deforming conditions (0 to 200 $\mu\text{m/s}$). Temporal fluctuations in the speckle patterns were quantified by exponential fitting of the normalized cross-correlation of sequential frames in each image series of speckle patterns to obtain the exponential decay time constant, τ . The decorrelation time constants of thin-cap fibroatheromas (TCFA) ($\tau=47.5\pm 19.2$ ms) were significantly lower than those of other atherosclerotic lesions ($P<0.001$), and the sensitivity and specificity of the LSI technique for identifying TCFA were $>90\%$. Speckle decorrelation time constants demonstrated strong correlation with histological measurements of plaque collagen ($R=0.73$, $P<0.0001$), fibrous cap thickness ($R=0.87$, $P<0.0001$), and necrotic core area ($R=-0.81$, $P<0.0001$). Under deforming conditions (10 to 200 $\mu\text{m/s}$), τ correlated well with cap thickness in necrotic core fibroatheromas ($P>0.05$).

Conclusions—The measurement of speckle decorrelation time constant from laser speckle images provides an index of plaque viscoelasticity and facilitates the characterization of plaque type. Our results demonstrate that LSI is a highly sensitive technique for characterizing plaque and identifying thin-cap fibroatheromas.

Keywords

atherosclerosis; diagnosis; imaging; lasers; plaque

The composition of atherosclerotic plaques is an important determinant in the progression of thrombus-mediated acute coronary syndromes.¹ Thin-cap fibroatheromas (TC-FAs) comprise the majority of coronary plaques implicated in acute coronary events.^{2,3} TCFA consist of a

thin fibrous cap (minimum cap thickness $<65 \mu\text{m}$), a large lipid-rich atheromatous core, and activated macrophages at the plaque shoulder.^{4,5} In addition to plaque morphology, the risk of plaque rupture is influenced by the mechanical properties of the atheroma. The accumulation of a compliant lipid pool influences the local stress distributions within the plaque and can result in rupture of the fibrous cap at focal weak points.^{6,7} In addition, the mechanical strength of atherosclerotic plaques is primarily determined by the fibrillar collagen content of the extracellular matrix, and collagen degradation is associated with an increased risk of plaque rupture.^{8,9}

Here, we investigate a new optical method, laser speckle imaging (LSI), for obtaining information about atherosclerotic plaque composition, morphology, and viscoelasticity. When temporally coherent light from a laser propagates through tissue, photons that undergo multiple scattering events traverse different optical path lengths before returning to the surface. Interference between photons returning from different regions within the tissue results in a granular intensity pattern on the tissue surface known as laser speckle.¹⁰ In a viscoelastic medium, suspended particles undergo Brownian motion, which is directly related to the viscoelastic properties of the medium.¹¹ Consequently, in TCFAs, because of the relatively low viscosity of the lipids, particles within a compliant necrotic core exhibit more rapid Brownian motion compared with stiffer fibrous regions of the plaque. Because scatterer motion causes a modulation of the laser speckle pattern, the measurement of temporal intensity variations should provide information about the intrinsic viscoelastic properties of the plaque and might be used to determine plaque composition and morphology.

A previous preliminary feasibility study using 5 aortic plaques indicated differences in laser speckle modulations between 2 necrotic core fibroatheromas, 1 with a thin fibrous cap and 1 with a thick fibrous cap.¹² Here, in a separate study, we investigate the capability of LSI for differentiating atherosclerotic plaque type and assessing plaque morphology and composition. Because the deformation of the coronary wall over the cardiac cycle may cause further modulation of the laser speckle pattern independently of plaque composition, we also investigate the influence of arterial deformation at physiological velocities on LSI measurements.

Methods

Specimens

A total of 118 aortic plaques from 14 human cadavers were studied. After harvest, the aortas were immediately stored in PBS at 4°C. The time between autopsy and imaging was 12 to 48 hours. Before imaging, the arteries were warmed to 37°C in PBS.

LSI

Laser speckle images of the aortic specimens were obtained with the optical setup shown in Figure 1a. Light (632.8 nm) from a helium-neon laser was reflected off a galvanometer-mounted mirror and focused to a 75- μm -diameter spot on the luminal surface of the specimen. The galvanometer-mounted mirror was computer controlled to provide scanning of the beam across the specimen. A CCD camera (TM-6710CL, Pulnix) was mounted above the aortic specimen and used to capture 2D speckle patterns at a rate of 240 frames per second for 2 seconds (Figure 1b). A polarizer was placed in front of the CCD camera lens to minimize specular reflections from the specimen surface.

Each specimen was clamped between 2 L brackets mounted on 2 separate linear motorized stages (Figure 1a). The L brackets were immersed in a PBS bath (37°C) such that the luminal surface of the specimen was exposed just above the level of PBS. The imaging site was marked

with 2 India ink spots to mark the diameter of the speckle pattern over the lesion, which ensured accurate registration with histopathology. To evaluate the efficacy of LSI for future in vivo coronary studies, we conducted LSI of aortic plaques during arterial deformation at velocities corresponding with the physiological range of coronary circumferential stretch.¹³ For the deformation experiments, 25 plaques were randomly selected. During imaging, aortic deformation was performed along the circumferential direction by stretching each specimen between the 2 opposing motorized stages at velocities between 10 and 200 $\mu\text{m/s}$.

Laser Speckle Analysis

Time-varying laser speckle patterns acquired under static and deforming conditions were analyzed using cross-correlation techniques to determine the speckle decorrelation time constant, τ , which is inversely related to the rate of change of the speckle pattern. The normalized 2D cross-correlation of the first speckle image with each image in the time-varying image series was computed in the Fourier domain.¹⁴ The normalized cross-correlation value was determined for each image and plotted as a function of time to obtain speckle decorrelation curves for each lesion. To estimate the rate of speckle decorrelation, τ was computed by exponential fitting of the normalized speckle decorrelation curve. Although speckle patterns were acquired over a 2-second duration, single exponential fitting was best performed in the region of the normalized speckle decorrelation curve over which the cross-correlation value dropped to 75% of its maximum. The time duration over which the cross-correlation value dropped to 75% of its maximum ranged from 40 ms for thin-cap fibroatheromas to 200 ms for fibrocalcific plaques (FCs).

Histopathological Characterization of Atherosclerotic Plaque

The imaged specimens were fixed in 10% formalin and subsequently processed, embedded, and sectioned using standard techniques. Sections were cut across the India ink marks; stained with hematoxylin-eosin, trichrome, picrosirius red (for collagen), and CD68 (for macrophages); and interpreted by a pathologist (G.J.T.) blinded to the LSI data. Subsequently, agreement on histopathological classification was analyzed between 2 pathologists (G.J.T. and S.L.H.) blinded to the LSI data. The histological sections were characterized on the basis of the classification scheme by Virmani et al⁴ into the following groups: necrotic core fibroatheroma, pathological intimal thickening (PIT) and nonnecrotic fibroatheroma (FA), intimal hyperplasia (IH), fibrous plaque, and FC. The necrotic core fibroatheromas were differentiated according to their fibrous cap thickness into TCFA (minimum cap thickness $<65 \mu\text{m}$) and thick-cap fibroatheromas (TKFA) (minimum cap thickness $\geq 65 \mu\text{m}$). Nonnecrotic FAs with dispersed extracellular lipid within the fibrous matrix were distinguished from PIT by an intimal thickness $>500 \mu\text{m}$. Because the PIT and IH groups did not represent discrete lesions, the subset of diagnostic lesions—TCFA, TKFA, FC, fibrous, and FA—were further categorized as atherosclerotic plaques.

Histopathological Analysis of Atherosclerotic Plaques

Total collagen content was determined in the atherosclerotic plaque groups using polarized light microscopy images of picrosirius red–stained sections within a 1.0×0.5 -mm (transverse times depth) region of interest (ROI) located between the fiducial ink marks. A hue transformation (IPLab Spectrum 3.9, Scanalytics) was performed, and collagen content was computed by dividing the number of hue values within a range of 0 to 180° (red-cyan) by the total pixel area of the ROI.^{15,16}

Histopathological measurements of fibrous cap thickness, necrotic core area, and macrophage content were performed on the TCFA and TKFA groups. The minimum fibrous cap thickness within the region between the fiducial ink marks was measured in the digitized trichrome-stained sections (IPLab Spectrum). Necrotic core area was measured by manually tracing the

necrotic core region contained within the central 1.0×0.5-mm ROI between the fiducial ink marks. Macrophage density was determined from CD68-stained digitized sections by first manually segmenting the region of the fibrous cap between the ink marks. The percentage area of CD68 staining within the fibrous cap region was then calculated using automated bimodal histogram thresholding and image segmentation.^{15,17}

Statistical Analysis

From histological diagnoses, the τ value associated with each lesion was assigned to 1 of 7 plaque groups. For each plaque type, the speckle decorrelation data were expressed as $\bar{\tau}+s_t$, where $\bar{\tau}$ is the average speckle decorrelation time constant computed for each plaque group and s_t is the standard deviation. The differences between measurements for all plaque groups were compared with 2-way (for plaque type and patient within each plaque group) ANOVA tests; the pairwise comparisons between multiple groups were evaluated by use of Dunnett's *t* test. A receiver-operating characteristic (ROC) curve analysis was used to evaluate the sensitivity and specificity of LSI for identifying TCFAs. To obtain the threshold value for τ , the sensitivity and specificity were determined and plotted for the entire range of time constant measurements, using each measurement as a diagnostic threshold. The τ value that provided both the highest sensitivity and specificity was selected as the optimum threshold for identifying TCFAs. The sensitivity, specificity, and area under the ROC curve were reported with 95% confidence intervals (CIs) (Medcalc statistical software, version 8.0). The interobserver and intraobserver agreements between pathologists for histopathological plaque classification were quantified by the κ test of concordance.¹⁸

For evaluation of plaque collagen content, necrotic core area, and macrophage content using LSI, we recalculated τ using a 1.0-mm×1.0-mm region in each speckle pattern centered at the illumination site. The relationships between τ and plaque collagen content, minimum fibrous cap thickness, necrotic core area, and macrophage content were investigated using linear regression. For all analyses, a value of $P<0.05$ was considered statistically significant.

Results

Atherosclerotic Plaque Characterization: Static Conditions

The aortic specimens were histologically classified as TCFA (n=14), TKFA (n=10), PIT (n=21), FA (n=22), IH (n=17), fibrous (n=28), and FC (n=6). The interobserver and intraobserver κ values between pathologists for differentiating necrotic core fibroatheromas, PIT, and FA, IH, fibrous, and FC lesions were $\kappa=0.58\pm0.06$ and $\kappa=0.68\pm0.05$, respectively. Figure 2a shows examples of the normalized speckle decorrelation curves computed under static conditions for 3 aortic specimens. As shown in Figure 2, TCFA demonstrated rapid speckle decorrelation ($\tau=28$ ms) compared with TKFA ($\tau=254$ ms) and fibrous plaque ($\tau=540$ ms). The average speckle decorrelation time constants computed for different plaque groups under static conditions are plotted in Figure 2b. The TCFA group had the lowest $\bar{\tau}$ (47.5 ± 19.2 ms), and the FC group had the highest $\bar{\tau}$ (685.0 ± 133.0 ms) compared with all the other plaque groups. The results of the ANOVA test demonstrated that differences in $\bar{\tau}$ between all the plaque groups were highly significant ($P<0.001$). The results of Dunnett's *t* test to compare pairwise differences in average speckle decorrelation time constant between multiple plaque groups are tabulated in Table 1, with the probability value reported in each case. We have controlled for multiple comparisons between plaque groups by performing Dunnett's *t* tests only after ascertaining that the probability value from the 2-way ANOVA test ($P<0.0001$) was significant. The IH, fibrous, and FC groups differed significantly from each of the other groups ($P<0.05$). The differences in $\bar{\tau}$ for the 3 plaque groups—TKFA, FA, and PIT—and that of other groups were highly significant ($P<0.05$); however, the differences between the 3 groups were not significant. The differences in average speckle decorrelation time constant for TCFA and each

of the plaque groups were highly significant ($P < 0.001$) in all cases. The sensitivity and specificity of LSI in identifying TCFA, evaluated at a threshold value of $\tau = 76.6$ ms were 100% (95% CI, 87% to 100%) and 92.3% (95% CI, 86% to 97%), respectively. The area under the ROC curve was 0.97 (95% CI, 0.92 to 0.97).

Figure 3 demonstrates the spatial distribution of τ as a function of beam location for 1 specimen measured by scanning the laser beam at 500- μm intervals over a distance of 4.5 mm. As the beam was scanned across the lesion, τ varied significantly depending on tissue type: τ was low (20 to 50 ms) in the necrotic core and higher (≈ 600 ms) in the predominantly fibrous regions (Figure 3). Figure 4 depicts a 2D color map of the spatial distribution of τ , measured by scanning the laser beam at 300- μm increments across a 4.5 \times 4.5-mm region containing a fibroatheroma. The fibroatheroma can be clearly identified in the color map as a well-demarcated region with a significantly lower τ relative to the surrounding aortic tissue. On visual inspection, the size and shape of the lesion in the color map agree well with the accompanying gross pathology.

Relationship Between Plaque Features and Laser Speckle Decorrelation

Plaque collagen content ranged from 0.2% for TCFA to 91% for fibrous plaque. In Figure 5a, total collagen content is plotted against τ all 74 plaques of the TCFA, TKFA, fibrous, and FA groups. Linear regression analysis showed good correlation between plaque collagen content and τ ($R = 0.73$, $P < 0.0001$). In Figure 5b, 5c, and 5d, τ is plotted against minimum cap thickness, necrotic core area, and macrophage content, respectively. Minimum fibrous cap thickness in necrotic core fibroatheromas ranged from 11 μm ($\tau = 21$ ms) to 406 μm ($\tau = 546$ ms). The necrotic core areas ranged from 0.03 mm^2 ($\tau = 40$ ms) to 0.47 mm^2 ($\tau = 369$ ms). Linear regression analysis demonstrated a high positive correlation between minimum cap thickness and τ ($R = 0.87$, $P < 0.0001$) and a strong inverse relationship between necrotic core area and τ ($R = -0.81$, $P < 0.0001$). Macrophage content measured from the CD68-stained sections ranged from 0.01% to 46% and did not demonstrate correlation with τ ($R = -0.2$, $P = 0.37$).

Atherosclerotic Plaque Characterization: Deforming Conditions

The rate of speckle decorrelation increased with deformation rate and was dependent on plaque type. Twelve of 25 aortic plaques, imaged during plaque deformation, were histologically classified as necrotic core fibroatheromas. Table 2 shows the results of linear regression analysis to determine the influence of stretch rate on decorrelation time constant for the necrotic core fibroatheromas. At each deformation rate under consideration, a strong positive correlation was demonstrated between τ and fibrous cap thickness ($P < 0.05$).

Table 3 summarizes the performance characteristics of LSI for the identification of necrotic core fibroatheromas (cap thickness < 100 μm) during arterial deformation with the sensitivity, specificity, and area under the ROC curve reported. A cap thickness of 100 μm was selected as the smallest cap thickness at which the τ value for necrotic core fibroatheromas was differentiable from other plaque groups during deformation ($P > 0.05$). The cap thickness threshold of < 65 μm could not be used in the deformation experiments because it was difficult to maintain the structural fidelity of very thin fibrous caps, which often fissured at high stretch velocities. Under deforming conditions, high sensitivity and specificity were achieved; even at the highest stretch rate of 200 $\mu\text{m}/\text{s}$, the sensitivity and specificity were 96% (95% CI, 89 to 100) and 95% (95% CI, 87 to 100), respectively, and the area under the ROC curve was 0.95 (95% CI, 0.79 to 0.99).

Discussion

We have described LSI, a new technique that measures the intrinsic Brownian motion of plaque molecules to provide an index of viscoelasticity.^{11,19} By analyzing time-varying laser speckle

patterns to calculate speckle decorrelation time constants, we have shown that the Brownian motion of scatterers within atherosclerotic plaques depends on plaque composition.

TCFAs exhibited a significantly higher rate of speckle decorrelation ($\tau \approx 47$ ms) compared with other more stable lesions as a result of rapid Brownian motion of particles within the compliant necrotic lipid pool ($P < 0.001$). As a result, the LSI technique demonstrated high diagnostic sensitivity (100%) and specificity (92%) for identifying TCFAs. Fibrous and fibrocalcific lesions were also easily discriminated from lipid-containing lesions because of their significantly higher time constants. We also found that LSI was sensitive to extracellular lipid content in FA and PIT lesions, resulting in a significantly lower τ (≈ 200 ms) compared with fibrous and FC plaques ($P < 0.0001$). In our analysis, 4 lesions, histologically confirmed to be FA and PIT, contributed to false positives for TCFAs. In these cases, regions of extracellular lipid in close proximity to the illumination location caused rapid speckle decorrelation, resulting in a lower τ .

We have also demonstrated the use of LSI in evaluating gross plaque morphology. By scanning the illumination beam over the lesion and computing τ at each beam location, we demonstrated that 2D maps can be reconstructed to evaluate the spatial variation in plaque viscoelasticity (Figure 4). Although scanning the beam provides a 2D representation of morphology within the probed volume, spatial variation in speckle fluctuations of the speckle pattern at each illumination location may be used to better distinguish plaque viscoelasticity as a function of depth. Monte Carlo simulation studies have shown that as light propagates through tissue, photons returning from deeper regions within the tissue have a higher probability of remittance farther away from the source beam entry point.^{20,21} By exploring this feature of LSI, in conjunction with beam scanning, it may be possible to obtain 3D volumetric maps of plaque viscoelasticity distributions. When analyzed in this manner, LSI specificity may be improved by better discriminating FA and PIT with superficial lipid from TCFA lesions.

LSI measures an index of viscoelasticity, and in our study we found the measurement of τ to be correlative with collagen content, fibrous cap thickness, and necrotic core area. LSI measurements of τ showed high correlation with plaque collagen content ($R = 0.73$, $P < 0.001$), and because fibrous cap thickness in necrotic core lesions is closely related to plaque collagen content, we similarly found a high correlation between τ and minimum cap thickness in these lesions ($R = 0.87$, $P < 0.001$). Likewise, a strong negative correlation ($R = -0.81$, $P < 0.0001$) was demonstrated between τ and necrotic core area. Plaque features such as collagen content, fibrous cap thickness, and necrotic core area are interrelated and contribute to the viscoelastic properties of the plaque. The data presented in Figure 5 suggest that the relationship between τ and plaque viscoelasticity may deviate from linearity and follow a more complex nonlinear model. However, the significant linear correlation does imply that the measures are highly related. Our data did not elucidate a relation between macrophage content and τ in necrotic core fibroatheromas, indicating that macrophage density may not directly influence plaque viscoelasticity. FC plaques were not included in the analysis of plaque collagen content because the speckle decorrelation rate was governed by the extent of calcification rather than the plaque collagen content in these lesions.

To evaluate the potential for LSI in patients, we investigated the behavior of laser speckle fluctuations during arterial deformation. LSI achieved high sensitivity and specificity in identifying necrotic core fibroatheromas with cap thickness $< 100 \mu\text{m}$, indicating that LSI may be used in vivo. At stretch velocities of 10 to 200 $\mu\text{m/s}$, we found that τ remained strongly correlated to fibrous cap thickness, suggesting that high-risk plaques may be identified during physiological coronary pulsation.

To extend LSI to patient studies, small-diameter flexible optical fiber bundles, similar to those of coronary angioscopy,²² could be used to launch laser light to the imaging tip and to obtain laser speckle images of coronary plaques. LSI can be performed safely with $<100 \mu\text{W}$ power incident on the vessel wall. As with other optical imaging techniques, the presence of blood could hinder accurate imaging of the arterial wall.²³ Intracoronary saline flushing has been successfully implemented in in vivo optical coherence tomography and angioscopy procedures in which a bolus of saline is injected to temporarily displace blood and completely fill the lumen between the imaging catheter and coronary wall, thus enabling unobstructed imaging of the coronary wall.²⁴⁻²⁶ Clinical studies using optical coherence tomography have shown that it is possible to completely purge the coronary lumen with saline during imaging to ensure that backscattering of light from blood cells is negligible.²⁴⁻²⁶ Likewise, this technique of intracoronary saline flushing may be used in conjunction with LSI to obtain intracoronary speckle images in vivo.

Study Limitations

Because cadaveric specimens were used in the study and were stored at 4°C in PBS before imaging, it is possible that minor degradation of the specimen may have occurred. Hence, it is possible that absolute measurements of τ obtained from ex vivo specimens may slightly vary under in vivo conditions. However, in the present study, because the differences in τ between the plaque groups were highly statistically significant ($P<0.0001$), we anticipate that these relative differences will be maintained under in vivo conditions.

During imaging, the luminal surface of the aortic specimen was exposed just above the level of PBS and not completely submerged within the bath. This was done to facilitate ink marking of the lesion site and to minimize laser speckle fluctuations occurring as a result of air currents above the PBS surface under in vitro conditions.

Registration of speckle images with corresponding histology was accomplished through the use of ink marks on the lesion site. Because tissue composition may vary as a function of measurement location, any errors in registration between speckle and histology images could affect our results. The estimation of collagen content, necrotic core area, and macrophage content was performed over a $1.0 \times 0.5\text{-mm}$ region in a single histology section obtained at the center of the lesion. However, the variation in these features over the measurement volume could influence the corresponding speckle pattern and potentially affect τ measurements.

The measurement of τ was performed by fitting a single exponential to the normalized speckle decorrelation data. However, the heterogeneous composition of atherosclerotic plaque may contribute to speckle decorrelation functions that are multiexponential in nature. By evaluating the contribution of the distributions of different decorrelation time constants, we may be able to increase the efficacy of LSI in investigating plaque heterogeneity.

During arterial deformation experiments, tissue slippage during deformation could occur, which may affect τ measurements. Tissue tearing at high deformation rates frequently occurred in FC plaques; as a result, these specimens were excluded from the deformation studies. Using our in vitro setup, we were unable to evaluate the efficacy of LSI in identifying TCFAs (cap thickness $<65 \mu\text{m}$ during deformation). We observed that aortic deformation at high stretch velocities caused thinning and fissuring of very thin fibrous cap during stretching, resulting in a small number of TCFAs analyzed in our deformation experiments. It is possible that extreme thinning of the fibrous cap, effects of minor tissue degradation during storage, and multiple stretching at high stretch rates of 10 to $200 \mu\text{m/s}$ may have contributed to fissuring of necrotic core fibroatheromas with very thin fibrous caps. The cap thickness of $100 \mu\text{m}$ was selected as the smallest cap thickness at which the identification of necrotic core fibroatheromas during deformation was achieved with statistical significance ($P<0.05$).

Under in vivo conditions, cyclic coronary deformation occurs in both the axial (longitudinal) and circumferential directions along the arterial wall. The cyclic arterial stretch is predominantly larger in the circumferential direction than in the axial direction, and we expect that the relatively small axial deformation would not significantly affect the correlation between speckle decorrelation time constants and plaque type. For this reason, we tested the influence of only circumferential stretch on LSI measurements.

In our study, although speckle images were acquired over a 2-second duration, measurements were performed by single exponential fitting of the region of the normalized speckle decorrelation curve over which the cross-correlation value dropped to 75% of its maximum. Under static conditions, this corresponded to an average acquisition time of 40 ms for TCFA and 200 ms for FC plaques. We expect that this relatively short acquisition time would allow for a sufficient temporal window during the resting phase of the cardiac cycle to obtain diagnostic quality speckle data by minimizing the influence of cardiac motion in vivo.

Other Plaque Characterization Methods

A variety of catheter-based imaging methods such as intravascular ultrasound, thermography, infrared spectroscopy, angioscopy, intravascular MRI, and optical coherence tomography have been investigated for the characterization of coronary plaque.^{12,22,24,27-34} These methods are complementary to techniques that measure biomechanical properties because they provide structural and compositional information that contributes to plaque stability. Intravascular ultrasound elastography facilitates atherosclerotic plaque characterization by computing local strains in the plaque in response to intraluminal pressure differentials exerted on the arterial wall.^{35,36} An optical method, laser strain gauge, has been described that evaluates laser speckle shifts to compute strains in arterial tissue resulting from an extrinsic applied load.³⁷ These techniques provide important information in that they afford the measurement of arterial response to a dynamic external loading environment, thus aiding the investigation of features contributing to plaque instability. However, measurement of plaque biomechanical properties with these approaches requires a priori knowledge of the microscopic plaque morphology and loading conditions to solve the inverse problem.

This study has demonstrated that the measurement of intrinsic Brownian motion of molecules within an atherosclerotic plaque from laser speckle images can be used to accurately distinguish plaque composition. Studies have shown that measurement of the time scale and mean square displacement of the trajectory of a particle can be used to calculate the viscoelastic modulus of polymer solutions.¹⁹ Using these principles, we could potentially calculate in future studies the intrinsic viscoelastic modulus of atherosclerotic lesions from LSI measurements independently of the evaluation of extrinsic mechanical stresses on the arterial wall.

Conclusions

LSI is unique in that it enhances plaque characterization by providing measurements that are related to the viscoelastic properties of atherosclerotic lesions. In doing so, at a single beam location, LSI enables identification of plaque type and measures an index of viscoelasticity that is related to plaque collagen content, fibrous cap thickness, and necrotic core area. Additionally, reconstruction of plaque morphology can be accomplished by scanning the illumination beam across the sample. Speckle images can potentially be obtained through catheter-based fiber bundles and therefore may be used as an independent tool or as a powerful adjunct to other optical techniques such as angioscopy. Given the wealth of information provided by this technique and its potential for intracoronary use, we anticipate that LSI will prove highly useful for the evaluation of high-risk coronary lesions.

CLINICAL PERSPECTIVE

The evaluation of plaque composition and viscoelasticity can provide valuable insight into intrinsic features associated with plaque rupture. The majority of atherosclerotic plaques implicated in thrombus-mediated acute coronary events are thin-cap fibroatheromas that comprise large compliant necrotic cores, mechanically weak, thin fibrous caps, and macrophages. This study introduces a new optical imaging technique called laser speckle imaging (LSI) to facilitate atherosclerotic plaque characterization and to enable the identification of thin-cap fibroatheromas with high diagnostic sensitivity and specificity. LSI is unique in that it measures the intrinsic Brownian motion of particles within the plaque to provide an index of viscoelasticity that is related to plaque composition. Using ex vivo studies on human cadaveric aortic plaques, the authors show that LSI measurements of particular Brownian motion are related to plaque collagen content, necrotic core area, and fibrous cap thickness. Additionally, by scanning the illumination beam, 2D maps of the spatial distribution of plaque viscoelasticity can be reconstructed that may be useful to identify potential sites of plaque rupture. Laser speckle images can potentially be obtained through catheter-based optical fiber bundles and therefore may be used as an independent tool or as a powerful adjunct to other optical techniques such as angioscopy. Given the wealth of information provided by this technique and its potential for intracoronary use, we anticipate that LSI will prove to be a highly useful method for the evaluation of high-risk coronary plaques.

Acknowledgments

This study was funded in part by the National Institutes of Health contract RO1-HL70039 and the Center for Integration of Medicine and Innovative Technology. Dr Nadkarni acknowledges financial support from the Natural Sciences and Engineering Research Council of Canada.

References

1. Falk E, Shah PK, Fuster V. Coronary plaque disruption. *Circulation* 1995;92:657–671. [PubMed: 7634481]
2. Kullo IJ, Edwards WD, Schwartz RS. Vulnerable plaque: pathobiology and clinical implications. *Ann Intern Med* 1998;129
3. Muller JE, Tofler GH, Stone PH. Circadian variation and triggers of onset of acute cardiovascular disease. *Circulation* 1989;79:733–743. [PubMed: 2647318]
4. Virmani R, Kolodgie FD, Burke AP, Farb A, Schwartz SM. Lessons from sudden coronary death: a comprehensive morphological classification scheme for atherosclerotic lesions. *Arterioscler Thromb Vasc Biol* 2000;20:1262–1275. [PubMed: 10807742]
5. Lee RT, Libby P. The unstable atheroma. *Arterioscler Thromb Vasc Biol* 1997;17:1859–1867. [PubMed: 9351346]
6. Richardson PD, Davies MJ, Born GV. Influence of plaque configuration and stress distribution on fissuring of coronary atherosclerotic plaques. *Lancet* 1989;2:941–944. [PubMed: 2571862]
7. Schroeder AP, Falk E. Vulnerable and dangerous coronary plaques. *Atherosclerosis* 1995;118 (suppl):S141–S149. [PubMed: 8821473]
8. Rekhter MD, Hicks GW, Brammer DW, Hallak H, Kindt E, Chen J, Rosebury WS, Anderson MK, Kuipers PJ, Ryan MJ. Hypercholesterolemia causes mechanical weakening of rabbit atheroma: local collagen loss as a prerequisite of plaque rupture. *Circ Res* 2000;86:101–108. [PubMed: 10625311]
9. Libby P, Aikawa M. Stabilization of atherosclerotic plaques: new mechanisms and clinical targets. *Nat Med* 2002;8:1257–1262. [PubMed: 12411953]
10. Goodman, JW. *Statistical Optics*. Vol. 2000. New York, NY: Wiley Interscience; p. 347-356.

11. Mason TG, Weitz DA. Optical measurements of frequency-dependent linear viscoelasticity moduli of complex fluids. *Phys Rev Lett* 1995;74:1250–1253. [PubMed: 10058972]
12. Tearney GJ, Bouma BE. Atherosclerotic plaque characterization by spatial and temporal speckle pattern analysis. *Optics Lett* 2002;27:533–535.
13. Ge J, Erbel R, Gerber T, Gorge G, Koch L, Haude M, Meyer J. Intravascular ultrasound imaging of angiographically normal coronary arteries: a prospective study in vivo. *Br Heart J* 1994;71:572–578. [PubMed: 8043342]
14. Lewis JP. Fast template matching. *Vision Interface* 1995:120–123.
15. Pratt, W. *Digital Image Processing*. 3. New York, NY: John Wiley and Sons, Inc; 2001.
16. Whittaker P, Kloner RA, Boughner DR, Pickering JG. Quantitative assessment of myocardial collagen with picosirius red staining and circularly polarized light. *Basic Res Cardiol* 1994;89:397–410. [PubMed: 7535519]
17. Tearney GJ, Yabushita H, Houser SL, Aretz HT, Jang IK, Schlendorf KH, Kauffman CR, Shishkov M, Halpern EF, Bouma BE. Quantification of macrophage content in atherosclerotic plaques by optical coherence tomography. *Circulation* 2003;107:113–119. [PubMed: 12515752]
18. Landis JR, Koch GG. The measurement of observer agreement for categorical data. *Biometrics* 1977;33:159–174. [PubMed: 843571]
19. Yamada S, Wirtz D, Kuo SC. Mechanics of living cells measured by laser tracking microrheology. *Biophys J* 2000;78:1736–1747. [PubMed: 10733956]
20. Gonik MM, Mishin AB, Zimnyakov DA. Visualization of blood micro-circulation parameters in human tissues by time-integrated dynamic speckles analysis. *Ann N Y Acad Sci* 2002;972:325–330. [PubMed: 12496036]
21. Sadhwani A, Schomacker KT, Tearney GJ, Nishioka NS. Determination of Teflon thickness with laser speckle, 1: potential for burn depth diagnosis. *Appl Optics* 1996;35:5727–5735.
22. Uchida Y, Fujimori Y, Hirose J, Oshima T. Percutaneous coronary angiography. *Jpn Heart J* 1992;33:271–294. [PubMed: 1522685]
23. Brezinski M, Saunders K, Jesser C, Li X, Fujimoto J. Index matching to improve optical coherence tomography imaging through blood. *Circulation* 2001;103:1999–2003. [PubMed: 11306530]
24. Jang IK, Bouma BE, Kang DH, Park SJ, Park SW, Seung KB, Choi KB, Shishkov M, Schlendorf K, Pomerantsev E, Houser SL, Aretz HT, Tearney GJ. Visualization of coronary atherosclerotic plaques in patients using optical coherence tomography: comparison with intravascular ultrasound. *J Am Coll Cardiol* 2002;39:604–609. [PubMed: 11849858]
25. MacNeill BD, Jang IK, Bouma BE, Iftimia N, Takano M, Yabushita H, Shishkov M, Kauffman CR, Houser SL, Aretz HT, DeJoseph D, Halpern EF, Tearney GJ. Focal and multi-focal plaque macrophage distributions in patients with acute and stable presentations of coronary artery disease. *J Am Coll Cardiol* 2004;44:972–979. [PubMed: 15337206]
26. Bouma BE, Tearney GJ, Yabushita H, Shishkov M, Kauffman CR, DeJoseph Gauthier D, MacNeill BD, Houser SL, Aretz HT, Halpern EF, Jang IK. Evaluation of intracoronary stenting by intravascular optical coherence tomography. *Heart* 2003;89:317–320. [PubMed: 12591841]
27. Liebson PR, Klein LW. Intravascular ultrasound in coronary atherosclerosis: a new approach to clinical assessment. *Am Heart J* 1992;123:1643–1660. [PubMed: 1595545]
28. Rogers WJ, Prichard JW, Hu YL, Olson PR, Benckart DH, Kramer CM, Vido DA, Reichek N. Characterization of signal properties in atherosclerotic plaque components by intravascular MRI. *Arterioscler Thromb Vasc Biol* 2000;20:1824–1830. [PubMed: 10894824]
29. Yabushita H, Bouma BE, Houser SL, Aretz HT, Jang IK, Schlendorf KH, Kauffman CR, Shishkov M, Kang DH, Halpern EF, Tearney GJ. Characterization of human atherosclerosis by optical coherence tomography. *Circulation* 2002;106:1640–1645. [PubMed: 12270856]
30. Brezinski ME, Tearney GJ, Bouma BE, Izatt JA, Hee MR, Swanson EA, Southern JF, Fujimoto JG. Optical coherence tomography for optical biopsy: properties and demonstration of vascular pathology. *Circulation* 1996;93:1206–1213. [PubMed: 8653843]
31. Schermund A, Rodermann J, Erbel R. Intracoronary thermography. *Herz* 2003;28:505–512. [PubMed: 14569392]

32. Stefanadis C, Toutouzas K, Tsiamis E, Pitsavos C, Papadimitriou L, Toutouzas P. Identification and stabilization of vulnerable atherosclerotic plaques: the role of coronary thermography and external heat delivery. *Ind Heart J* 2001;53:104–109.
33. Casscells W, Hathorn B, David M, Krabach T, Vaughn WK, McAllister HA, Bearman G, Willerson JT. Thermal detection of cellular infiltrates in living atherosclerotic plaques: possible implications for plaque rupture and thrombosis. *Lancet* 1996;347:1447–1451. [PubMed: 8676628]
34. Moreno PR, Lodder RA, Purushothaman KR, Charash WE, O'Connor WN, Muller JE. Detection of lipid pool, thin fibrous cap, and inflammatory cells in human aortic atherosclerotic plaques by near-infrared spectroscopy. *Circulation* 2002;105:923–927. [PubMed: 11864919]
35. de Korte CL, van der Steen AF, Cespedes EI, Pasterkamp G. Intravascular ultrasound elastography in human arteries: initial experience in vitro. *Ultrasound Med Biol* 1998;24:401–408. [PubMed: 9587995]
36. Schaar JA, De Korte CL, Mastik F, Strijder C, Pasterkamp G, Boersma E, Serruys PW, Van Der Steen AF. Characterizing vulnerable plaque features with intravascular elastography. *Circulation* 2003;108:2636–2641. [PubMed: 14581406]
37. Kirkpatrick SJ, Cipolla MJ. High resolution imaged laser speckle strain gauge for vascular applications. *J Biomed Opt* 2000;5:62–71. [PubMed: 10938768]

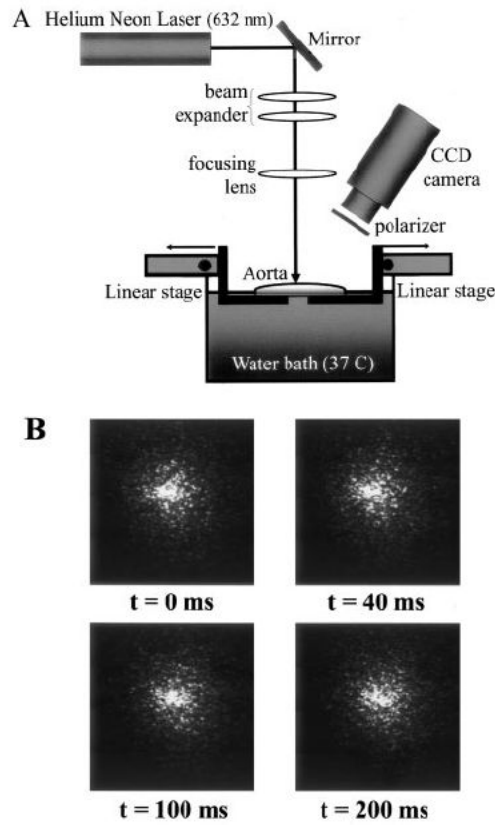


Figure 1.

a, Experimental setup to acquire laser speckle patterns from excised human cadaveric aortas. Time-varying speckle patterns were obtained during both static and deforming states of tissue. Arterial deformation was incorporated by stretching aorta between 2 opposing linear stages.

b, Speckle patterns acquired from aortic TCFA lesion at different time points showing time-dependent fluctuation of laser speckle.

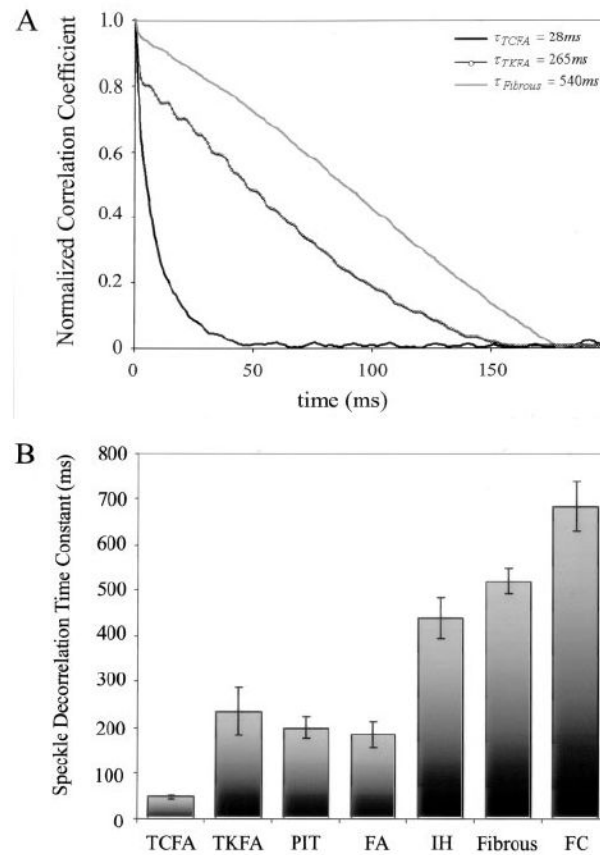


Figure 2.

a, Speckle decorrelation curves obtained for 3 aortic specimens: TCFA, TKFA, and fibrous aortic plaques. b, Average decorrelation time constants computed for different atherosclerotic plaque groups under static conditions. Error bars indicate SEM.

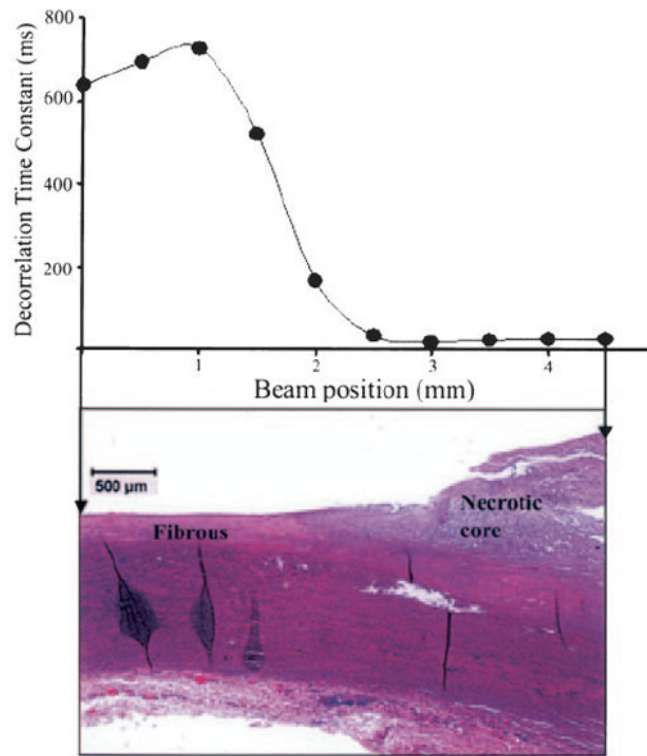


Figure 3. Variation in time constant τ as illumination beam scans across lesion from fibrous tissue to lipid-rich necrotic region.

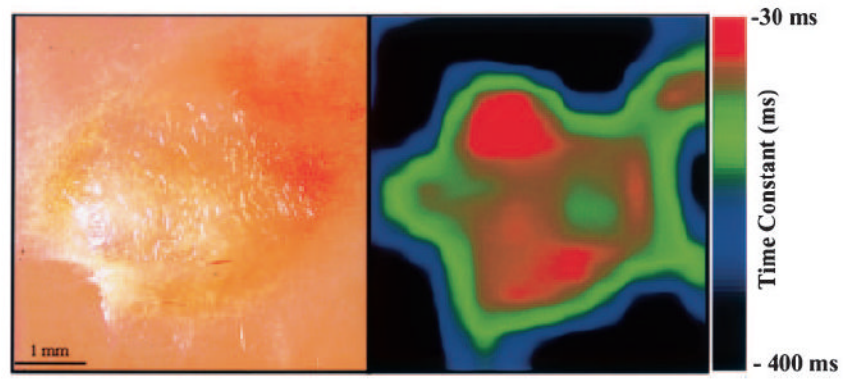


Figure 4. Color map of distribution of τ (30 to 400 ms) over 4.5×4.5-mm ROI across lesion. Presence of lipid-rich plaque with clearly demarcated borders is evident in color map and is corroborated in accompanying gross pathology photograph.

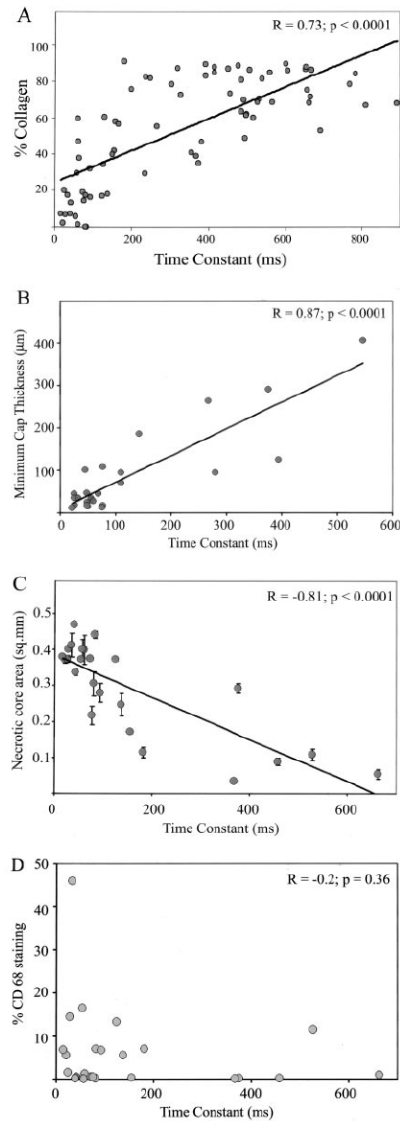


Figure 5.

Relation between plaque features and speckle decorrelation time constant τ a, High positive correlation is demonstrated between τ and plaque collagen content for TCFA, TKFA, fibrous, and FA lesions ($R=0.73$, $P<0.0001$). b, Strong positive correlation is demonstrated between τ and fibrous cap thickness for TCFA and TKFA lesions ($R=0.87$, $P<0.0001$). c, Strong negative correlation is demonstrated between τ and necrotic core area for TCFA and TKFA lesions ($R=-0.81$, $P<0.0001$). d, No correlation was demonstrated between τ and macrophage density of TCFA and TKFA lesions ($R=-0.2$, $P=0.36$).

TABLE 1

Atherosclerotic Plaque Characterization Using LSI: Differences in τ for Different Plaque Groups Under Static Conditions

	<i>P</i> Value					
	TKFA	TKFA	PIT	FA	IH	Fibrous
TKFA	<0.001
PIT	<0.0001	0.8059
FA	<0.0003	0.7931	0.5248
IH	<0.0001	<0.02	<0.02	<0.003
Fibrous	<0.0001	<0.0001	<0.0001	<0.0001	<0.05	...
FC	<0.0001	<0.0001	<0.0001	<0.0001	<0.001	<0.01

P<0.05 is considered statistically significant.

TABLE 2

Relation Between Speckle Decorrelation Time Constant and Minimum Cap Thickness of Necrotic Core Fibroatheromas Under Deforming Conditions

Deformation Rate, $\mu\text{m/s}$	<i>R</i>	<i>P</i>
0	0.85	<0.001
10	0.72	<0.01
20	0.81	<0.01
50	0.76	<0.01
100	0.73	<0.01
200	0.65	<0.02

TABLE 3

Deforming Conditions: Performance of LSI in Identifying Necrotic Core Fibroatheromas (With Minimum Cap Thickness <100 μm)

Stretch Velocity, $\mu\text{m/s}$	τ Cutoff, ms	Area Under ROC Curve	Sensitivity, %	Specificity, %
10	66.5	0.98 (0.83–1.0)	95 (86–100)	96 (88–100)
20	55	0.98 (0.83–1.0)	96 (89–100)	95 (87–100)
50	35	0.92 (0.74–0.99)	97 (90–100)	82 (67–97)
100	12.5	0.99 (0.86–1.0)	99 (95–100)	99 (95–100)
200	9.75	0.95 (0.79–0.99)	96 (89–100)	95 (87–100)

Numbers within parentheses are 95% CIs.